Evaluation of Physicochemical and Amphiphilic Properties of New Xanthan Gum Hydrophobically Functionalized Derivatives

Madiha Melha Yahoum, Selma Toumi, Hichem Tahraoui, Sonia Lefnaoui, Abdelkader Hadj-Sadok, Abdeltif Amrane, Mohammed Kebir, Jie Zhang, Aymen Amine Assadi, Lotfi Mouni

sustainability

MDPI

Article

Evaluation of Physicochemical and Amphiphilic Properties of New Xanthan Gum Hydrophobically Functionalized Derivatives

Madiha Melha Yahoum [1], Selma Toumi [2], Hichem Tahraoui [3,4,*], Sonia Lefnaoui [5], Abdelkader Hadjsadok [6], Abdeltif Amrane [7,*], Mohammed Kebir [8], Jie Zhang [9], Aymen Amine Assadi [7,10] and Lotfi Mouni [11]

1 Materials and Environmental Laboratory (LME), University of Medea, Nouveau Pole Urbain, Medea 26000, Algeria
2 Faculty of Sciences, University of Medea, Nouveau Pole Urbain, Medea 26000, Algeria
3 Laboratoire de Génie des Procédés Chimiques, Department of Process Engineering, University of Ferhat Abbas, Setif 19000, Algeria
4 Laboratory of Biomaterials and Transport Phenomena (LBMTP), University Yahia Fares, Medea 26000, Algeria
5 Laboratory of Experimental Biology and Pharmacology, University of Medea, Nouveau Pole Urbain, Medea 26000, Algeria
6 Functional Analysis of Chemical Processes Laboratory, Chemical Engineering Department, Saad Dahlab University, BP 270, Blida 09000, Algeria
7 Ecole Nationale Supérieure de Chimie de Rennes, Centre National de la Recherche Scientifique (CNRS), ISCR—UMR 6226, Université de Rennes, F-35000 Rennes, France
8 Research Unit on Analysis and Technological Development in Environment (URADTE-CRAPC), BP 384, Bou-Ismail, Tipaza 42004, Algeria
9 School of Engineering, Merz Court, Newcastle University, Newcastle upon Tyne NE1 7RU, UK
10 College of Engineering, Imam Mohammad Ibn Saud Islamic University, IMSIU, Riyadh 11432, Saudi Arabia
11 Laboratory of Management and Valorization of Natural Resources and Quality Assurance, SNVST Faculty, Akli Mohand Oulhadj University, Bouira 10000, Algeria
* Correspondence: hichemm.tahraouii@gmail.com (H.T.); abdeltif.amrane@univ-rennes1.fr (A.A.)

Citation: Yahoum, M.M.; Toumi, S.; Tahraoui, H.; Lefnaoui, S.; Hadjsadok, A.; Amrane, A.; Kebir, M.; Zhang, J.; Assadi, A.A.; Mouni, L. Evaluation of Physicochemical and Amphiphilic Properties of New Xanthan Gum Hydrophobically Functionalized Derivatives. *Sustainability* **2023**, *15*, 6345. https://doi.org/10.3390/su15086345

Academic Editor: Marko Vinceković

Received: 25 February 2023
Revised: 20 March 2023
Accepted: 27 March 2023
Published: 7 April 2023

Abstract: This research aimed to develop new hydrophobic and potentially amphiphilic benzyl xanthan gum (BXG) derivatives using a Williamson synthesis. This modification consists of an etherification reaction between xanthan gum (XG) and benzyl chloride (BC) under microwave heating. The effects of the molar ratio (R = XG/CLB, with R equal to 2 or 4) on the amphiphilic character and the degree of substitution (DS) were studied. The two benzyl xanthan gum derivatives (BXG1 and BXG2) were subsequently subjected to various physicochemical and rheological characterization techniques. The obtained results of FTIR and H^1-NMR spectroscopy showed the effectiveness of the grafting of aromatic moieties onto the XG molecule with DS values of 0.59 for BXG1 and 0.7 for BXG2. The XRD analysis revealed slight modifications in the xanthan crystallinity after etherification, where the degree of crystallinity (DOC) values were 8.46%, 10.18%, and 14.67% for XG, BXG1, and BXG2, respectively. Additionally, conductivity measurements showed that the BXG derivatives exhibit higher values than native XG, due to the inter- and intra-molecular associations following the grafting of aromatic groups. Moreover, the critical aggregation concentration (CAC) was detected at 0.32% for BXG1 and 0.28% for BXG2. The rheological study confirmed that XG and its BXG derivatives exhibited a shear-thinning pseudoplastic behavior and that the viscosity increases when the DS increases. The emulsifying power test of the BXGs compared to the native XG confirmed the amphiphilic properties of the new benzylated derivatives, where the stabilizing capacity increases with increased DS.

Keywords: xanthan gum; benzyl chloride; Williamson synthesis; benzyl xanthan gum; amphiphilic polysaccharides; oil in water emulsions

1. Introduction

Polysaccharides are defined as polymeric carbohydrate structures composed of repeating monosaccharide units that are joined by glycosidic bonds. Polysaccharides exhibit excellent physicochemical properties in terms of thickening, suspending, emulsifying, and stabilizing [1]. These macromolecules are generally hydrophilic and water-soluble. As natural biopolymers, polysaccharides are stable, non-toxic, biocompatible [2], and biodegradable [2,3]. Polysaccharides have many fields of application ranging from the food industry [4,5] and medical and pharmaceutical fields [6,7] to oil drilling [8]. However, polysaccharides also have some drawbacks, thus limiting their range of application. Among these disadvantages, the most commonly cited are inappropriate mechanical properties, unstable viscosity, and low shear strength, making them unsuitable for many applications such as emulsification [9]. They have several resources such as algae, like carrageenans [10], plants such as cellulose, or micro-organisms such as dextran and xanthan gum [11].

Among microbial polysaccharides, xanthan gum is an extracellular pentasaccharide secreted by the fermentation process of *Xanthomonas compestris* micro-organisms. It is known for its high molecular weight and high solubility in cold water. In addition, it exhibits a high pseudoplastic flow. The primary structure of this interesting biomaterial consists of 1,4-linked glucose residues (cellulose-like backbone) attached to a trisaccharide side chain by the carbon C-3, containing two mannose units separated by a glucuronic acid unit. The inner mannose unit consists of an acetyl residue at C-6 while the outer one is connected to a pyruvic acid residue (C-4) [12]. Because of its exceptional rheological behavior, xanthan gum is widely employed as a thickener, gelling agent, and emulsion stabilizer in an extended range of applications such as cosmetics, especially as a thickener in toothpaste and creams, and in the pharmaceutical and medical fields as a suspending and emulsifying agent [13], and also in oil recovery by the polymer flooding process as an additive in petroleum drilling fluids [14]. Although xanthan gum (XG) is very useful in its native form, however, it should be emphasized that it presents a lot of drawbacks that limit its use in many applications. This is why it is often necessary to improve its physicochemical properties by functionalization using a chemical modification to expand its range of use.

Several studies on the chemical modification of xanthan gum by various techniques and the grafting of different groups are described in the literature [11,15–18]. The nature of the grafted groups differentiates the structural characteristics of the polysaccharides due to various physicochemical and biological properties [19]. However, the hydrophobic modification of xanthan gum has been rarely studied. Only a few studies exist on the development of hydrophobically modified amphiphilic xanthan derivatives [20].

Fantou et al. [21] synthesized a chemically modified xanthan by an amidation reaction with the grafting of octylamine groups onto the carboxylic acid function of XG.

A xanthan gum hydrophobically modified derivative was also developed by Quan et al. [22], where hydrophobic carbon chains (C16) were grafted onto the hydrophilic backbone of xanthan gum in an N-dimethylformamide (DMF) solution. Sara et al. [23] performed the synthesis of new alkylated derivatives of xanthan by an etherification reaction with octyl chloride. The amphiphilic octyl xanthan derivatives presented interesting physicochemical characteristics and emulsifying proprieties. More shear-resistant xanthan derivatives were obtained by Wang et al. [24], using an esterification reaction with poly (maleic anhydride/1-octadecene) in a dimethyl sulfoxide solution.

Zhen et al. [25] reported that hydrophobically modified polysaccharides displayed stronger assembling tendencies to form multimolecular self-aggregates. Owing to intra- and/or inter-molecular hydrophobic interactions, the amphiphilic polysaccharides can self-associate in aqueous solution [19]. The formation of self-aggregates, including micelles, was dependent on the structural parameters of the modified polymer and their environmental conditions. Their formation was mainly driven by intermolecular interactions of hydrophobically modified polysaccharides such as hydrophobic, hydrogen-bonding, and electrostatic interactions.

Amphiphilic polysaccharides are generally used for applications in many fields such as the pharmaceutical, cosmetics, or food industries and other fields. Then, it is important to improve the techniques of synthesis to reach the "green label" using the application of green chemistry principles, as much as possible, which contributes to the development of sustainable and cost-effective methods. Indeed, this leads to the obtention of safer products for health and contributes to an improvement in the environmental impact of these processes [26]. The use of natural polymers in combination with an eco-friendly process based on microwave irradiation and the replacement of organic solvents, which potentially present toxic, environmental, or health hazards, by a harmless solvent falls within this perspective [27–29]. The application of greener modification processes to xanthan gum remains rare.

Only two recent works have reported the greener synthesis of novel hydrophobically modified xanthan derivatives. Mira et al. [30] reported the development of new functionalized xanthan gum derivatives by esterification using various alkenyl succinic anhydrides in green media. Surface active alkenyl, dodecenyl and hexadecenyl succinic-grafted xanthan derivatives were obtained. The thermal decomposition of the amphiphilic alkylated xanthan derivatives as well as their intrinsic properties and rheological behavior in aqueous media were also investigated by Mira et al., 2023 [31].

Until now, among all the modifications that have been reported on xanthan, none have been related to the grafting of benzyl groups, in particular under microwaves. The particularity of the benzyl groups lies in the fact that aromatic rings are commonly involved in Van der Waals and good hydrophobic interactions [32].

Moreover, this type of derivative, which is particularly interesting, will find potential applications in various fields such as that of oil recovery, knowing that aromatic compounds are the third major group of hydrocarbons commonly found in crude oil [33] or even the pharmaceutical field for the encapsulation or dispersion of hydrophobic active substances, knowing that a good number of active principles contain an aromatic ring [32]. Another potential application of such benzyl derivatives is the stabilization of hydrophobic nanoparticle dispersions in aqueous media by preventing their agglomeration through steric stabilization via hydrophobic interactions, as reported by Skender et al. [34], where the dispersibility of double-walled carbon nanotubes suspensions was improved by three derivatives of xanthan gum obtained by the grafting of aromatic hydrophobic moieties with Diphenylmaleic anhydride, Phthalic anhydride, and Epichlorhydrin-Phenoland.

The objective of this work, which may be considered as a first, aims to chemically modify native xanthan gum (XG) using a Williamson etherification synthesis (Figure 1) for the grafting of hydrophobic benzyl groups onto its backbone to transform it from a completely hydrophilic macromolecule into an amphiphilic one. Several characterization techniques were employed to determine the effect of the molar ratio on the degree of substitution (DS) and the physicochemical and rheological properties of the new derivatives. In addition, the emulsifying power has been evaluated to demonstrate that the developed benzyl xanthan gum derivatives can be used in various formulations as amphiphilic biopolymers instead of certain expensive biopolymers or to replace certain synthetic polymers and surfactants.

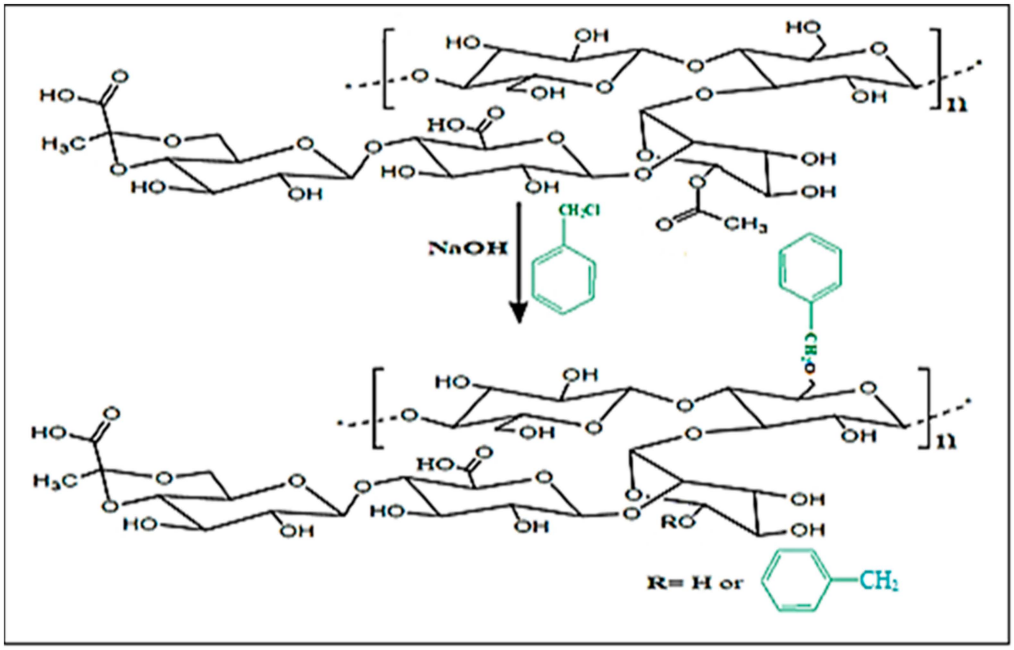

Figure 1. Chemical modification of xanthan gum (XG) by etherification reaction with benzyl chloride.

2. Materials and Methods

2.1. Materials

Xanthan gum (XG) was kindly donated by Saidal group (Medea, Algeria) and cold-pressed black seed oil (BSO) was procured from Abu El Kassim industries (Algiers, Algeria). The benzyl chloride (BC) ($C_6H_5CH_2Cl$, 99%, Sigma Aldrich, Hamburg, Germany), sodium hydroxide (NaOH, 98.5%, Sigma Aldrich, Hamburg, Germany), and acetic acid (CH_3COOH, 99.5%, Sigma Aldrich, Hamburg, Germany) and all other chemical products used in all of the experimental procedures were of analytical grade.

2.2. Methods

Hydrophobic Modification of Xanthan Gum

The etherification reaction of XG was carried out according to the procedure described by Yahoum et al. [11] with few changes. An amount of native xanthan gum was dispersed in 100 mL of distilled water using a magnetic agitator. Then, 5 mL of NaOH aqueous solution (16N) was added dropwise to the dispersion with continuous stirring (1 mL every 15 min). After that, a necessary volume of the reactant (BC) corresponding to the molar fraction (R) of (reagent/monomer) = 2 or 4 was added dropwise and then the reactional mixture was introduced for 1 min in the microwave oven (SAMSUNG MS23F301TAW, 2.45 GHz, Kuala Lumpur, Malaysia) at 180 W to obtain the two derivatives BXG1 and BXG2. The BXG derivatives were first neutralized using acetic acid before being recovered by precipitation from a hydro-alcoholic solution containing 80% ethanol and then vacuum-filtered with repeated washings. Finally, the solid obtained was dried at (70 ± 0.5) °C for 24 h and finely crushed in a glass mortar, and then submitted for several physicochemical tests.

2.3. Evaluation of BXGs Physicochemical Proprieties

2.3.1. Fourier Transform Infrared Study (FTIR) and the Degree of Substitution (DS)

For the FTIR analysis, the samples of native xanthan (XG) and its two derivatives BXG1 and BXG2 were ground with potassium bromide in an agate mortar before being pressed together to obtain translucent KBr pellets, which were analyzed using an FT-IR spectrometer (FTIR-8400 SHIMADZU, Tokyo, Japan). The spectra of the samples were recorded in the range of wavelengths varying from 400 cm^{-1} to 4000 cm^{-1} at a resolution

of 4 cm^{-1} (10 scans). The degree of substitution for the BXG derivatives was determined according to the previously reported method by Ming-Fei et al. [35] as follows:

$$DS = I \frac{A_1(-CH \text{ of aromatic cycle})}{A_2(-CH \text{ of methyl group})} \quad (1)$$

where A represents the area that refers to the absorbance determined by FTIR, while A_1 is determined at 864.77 cm^{-1} and A_2 is between 2900 and 2800 cm^{-1}.

2.3.2. ^{1}HNMR Analysis

^{1}H NMR spectroscopic testing was carried out in a Bruker ^{1}H NMR spectrometer 400 Hz (Ettlingen, Germany). The dry powdered samples of XG, BXG1, and BXG2 were first dissolved in deuterium oxide (D_2O) and then the ^{1}H NMR spectra of each biopolymer were recorded at 30 °C. Then, the results obtained were analyzed using MestReNova software (Version 2.9) for all the samples.

2.3.3. Morphological Analysis

Scanning electron microscopy (SEM) was used for the morphological examination of XG and its BXG derivatives. The analysis was performed at 25 °C using a scanning electron microscope (FEI Quanta 250) connected to an xT microscopy software for data analysis. All samples were observed at an accelerating potential of 15 kV at 3000 and 6000-fold magnifications.

2.3.4. X-ray Diffraction (XRD)

The XRD analysis of the samples was performed in a Bruker D2 PHASER diffractometer (Karlsruhe, Germany), in which each dry powdered sample was scanned and the diffraction patterns were recorded in the range of diffraction angles varying between 15° and 80° (2θ). Then, the Match3 software was used for the degree of crystallinity (DOC) calculation using the following formula:

$$DOC = \left(\frac{A_c}{A_C + A_a} \right) \times 100 \quad (2)$$

where A_c is the area of the diffraction peaks that correspond to the crystalline phase, and A_a is the area of the peaks that correspond to the amorphous phase. The DOC represents the fraction of the material that is in a crystalline form.

2.3.5. Rheological Study

Rheological studies were performed using an Anton Paar rheometer equipped with a cone and plate measuring device (angle 1°, 60 mm diameter) at (25 ± 0.5) °C. Polymer solutions of XG and BXGs were prepared by the dispersion of a given amount of polysaccharide (0.5% and 1%, *w*/*v*) in water under magnetic stirring. The obtained solutions were then allowed to rest for 24 h before use. The flow curves of XG and BXGs, describing the apparent viscosity variation versus shear rate, were determined in the interval of 0.001–1000 s^{-1}. The viscoelastic study was carried out by recording the variation of the storage (G′) and loss (G″) moduli with deformation between 0.1 and 1000% at a frequency value of 1 Hz.

2.3.6. Viscosity-Average Molecular Weight Determination

The molecular weight determination of xanthan gum and BXGs was carried out by the viscosimetric technique at concentration values at which both xanthan gum and its benzyl derivatives are in the dilute regime and behave as Newtonian fluids, as previously described by Masuelli [36] using an Ubbelhode viscometer at the temperature of 25 ± 0.1 °C [37]. A stock solution was first prepared by dissolving a quantity of polymer sample (0.27 g) in 200 mL of sodium chloride (NaCl) solution (0.01 M). For each polymer sample, two diluted

solutions at the concentrations of 0.01 and 0.075% were prepared from this stock solution of native XG, BXG1, and BXG2.

The Mark–Houwink empirical Equation (3) was then used for the calculation of the average molecular weight from the intrinsic viscosity [η] as follows:

$$[\eta] = k \cdot M^a \quad (3)$$

with: k = 2.79 10^{-3} cm^3/g and a = 1.2754 at 25 °C [38].

2.3.7. Critical Aggregation Concentration by Conductivity Measurements

The critical aggregation concentrations (CAC) of the BXG derivatives were determined by a conductivity study. Different solutions of BXG1 and BXG2 were prepared at concentrations varying from 0.01 to 1% (*w*/*v*) and conductivity was measured using a JP Selecta conductivity meter. All of the measurements were performed in triplicate.

2.3.8. Emulsifying Study

Emulsion Preparation

An emulsification test was carried out to study the stabilizing capacity of the new BXG hydrophobic derivatives. For this purpose, oil/water (O/W) surfactant-free emulsions stabilized by XG and BXGs were formulated as described by Shahin et al. [39] where the oily phase of the emulsions consists of natural black seed oil (BSO) at the fraction of 20% (*w*/*v*) and the aqueous phase is composed of XG, BXG1, and BXG2-based aqueous solutions at 0.5 and 1% *w*/*v* (Table 1). The two phases were subjected to heating separately at (60 ± 0.5) °C. Then, the oily phase was introduced fraction-wise to the aqueous phase under vigorous magnetic stirring, until a homogeneous mixture was obtained. After that, the pre-emulsions were homogenized at 10,000 rpm for 5 min using an Ultraturax IKA Homogenizer and left to rest for 24 h.

Table 1. Composition of the formulated emulsions.

Composition	F1	F2	F3
BSO (%)	20	20	20
XG (%)	1	-	-
BXG1 (%)	-	1	-
BXG2 (%)	-	-	1
Water (%)	79	79	79

Macroscopic and Microscopic Assessments

The macroscopic appearance of the formulated o/w emulsions was assessed by a visual appreciation of their color, homogeneity, and consistency, immediately after their preparation and after 24 h.

The emulsions' microscopic structures were examined using a Micros MCX10 optical microscope.

2.3.9. Statistical Assessment

All experimental measurements were conducted in triplicate (n = 3). The obtained experimental results are expressed as mean ± standard deviation error (SD). Statistical analysis was carried out with Tukey's one-way comparison tests (ANOVA) at a confidence interval of 95% ($p < 0.05$), using OriginPro 9 software.

3. Results and Discussion

3.1. FTIR Analysis

The Fourier Transform Infrared Spectroscopy (FTIR) spectra of xanthan gum (XG) and its novel XGB derivatives are illustrated in Figure 2. Both XG and BXGs spectra showed the appearance of the peaks at 1022.36 cm^{-1}, 1407.24 cm^{-1}, and 1626.12 cm^{-1}, respectively,

corresponding to the stretching of ether function (-C-O-C), the methyl vibration (C-H), and asymmetric stretching of carboxylic groups. The characteristic peak at 1717 cm^{-1}, which is inherent to acetyl group stretching for XG, disappeared on the spectra of BXGs, which is currently attributed to the deacetylation of the polysaccharides under strongly alkaline conditions [9,10]. The peak assigned to the elongations of the hydroxyl (-OH) group was detected at 3315.79 cm^{-1} [11,40]. In addition, it was observed that the intensity of this peak decreased for XGB derivatives, which confirmed the substitution of the (-OH) groups.

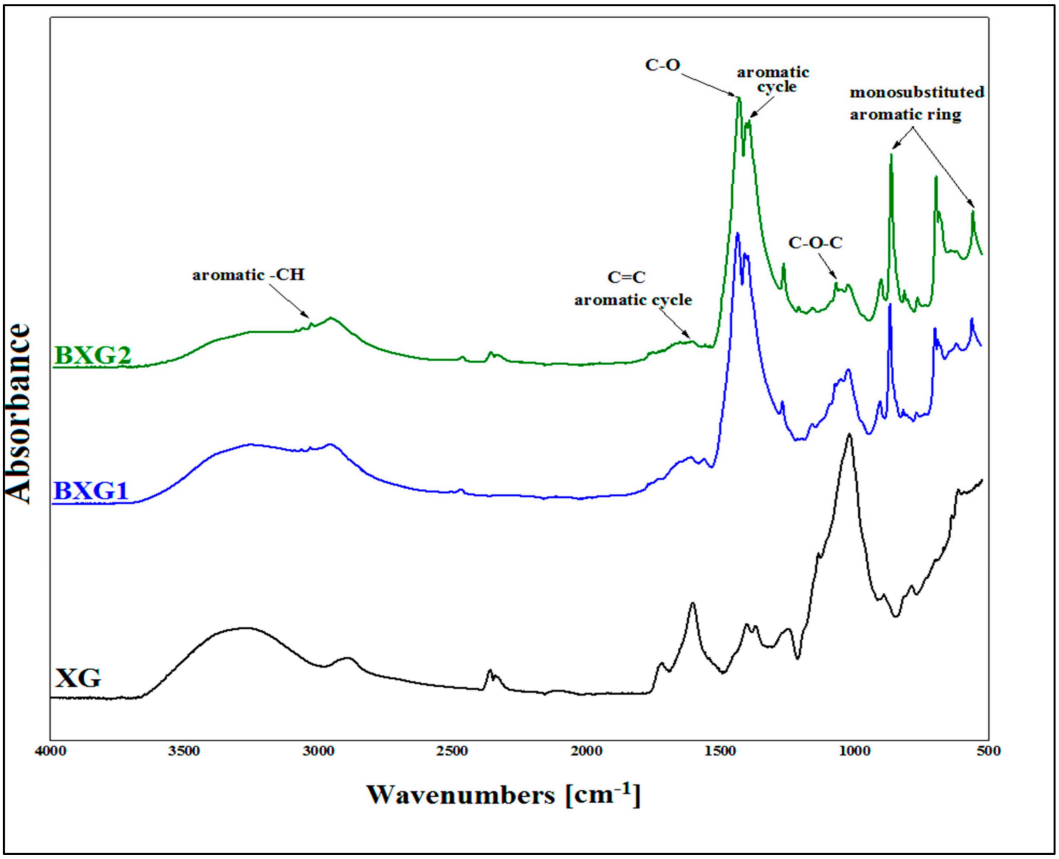

Figure 2. FTIR spectra of native XG and BXGs.

The appearance of new symmetrical bands on the BXGs spectra was also observed at 563.54 cm^{-1} and 864.77 cm^{-1}, corresponding to the monosubstituted aromatic ring and which, the intensity was more pronounced for BXG2 [41], as well as the peak at 1439.53 cm^{-1}, corresponding to the aromatic cycle [11]. The peak at 1110 cm^{-1} for the BXG1 and BXG2 is characteristic of the ether function, which was more intense for BXG2. The peak at 1612 cm^{-1} corresponds to the C=C functions of the aromatic cycle [41], as well as the appearance of a peak at 1452 due to the formation of the C-O (ether) bond, which is of greater intensity in the case of BXG2 and, finally, the new mean-intensity elongation observed at 3036 cm^{-1}, which is characteristic of aromatic -CH groups and whose intensity increases as a function of the degree of modification, in addition to the decrease in the intensity of the hydroxyl band, confirming the modification of xanthan gum.

The results of the DS determination indicated a significant difference ($p < 0.05$) in the DS values between the two derivatives and that the derivative BXG2 presented a higher DS value (DS = 0.70) compared with BXG1 (DS = 0.59). These findings indicate that the higher the molar ratio R, the higher the DS values are ($p < 0.05$). The increase in the degree of substitution with R can be attributed to the availability of more additional benzyl groups that are accessible to the grafting sites, thus increasing the percentage of grafting ($p < 0.05$).

Similar results were reported by Desbrières et al. [27] for the grafting of Plantago psyllium husk (psy) with Glycidyl methacrylate under microwave heating.

3.2. ^{1}HNMR Analysis

^{1}H-NMR analysis was carried out to confirm the successful hydrophobic modification of native xanthan gum. The spectra of XG and its derivatives are shown in Figure 3, where the appearance of a large peak at 4.7 ppm was detected, which corresponds to the anomeric proton overlapped by deuterium oxide (D_2O) solvent. The XG spectrum showed apparent peaks at 1.87 ppm, which are attributed to the acetyl groups [11,42] and the peak that corresponds to the glucuronic acid proton was observed at 2.02 ppm [42]. Additionally, the peak related to the alcoholic proton -CH_2 (-CH_2-OH) was detected at 3.17 ppm [11].

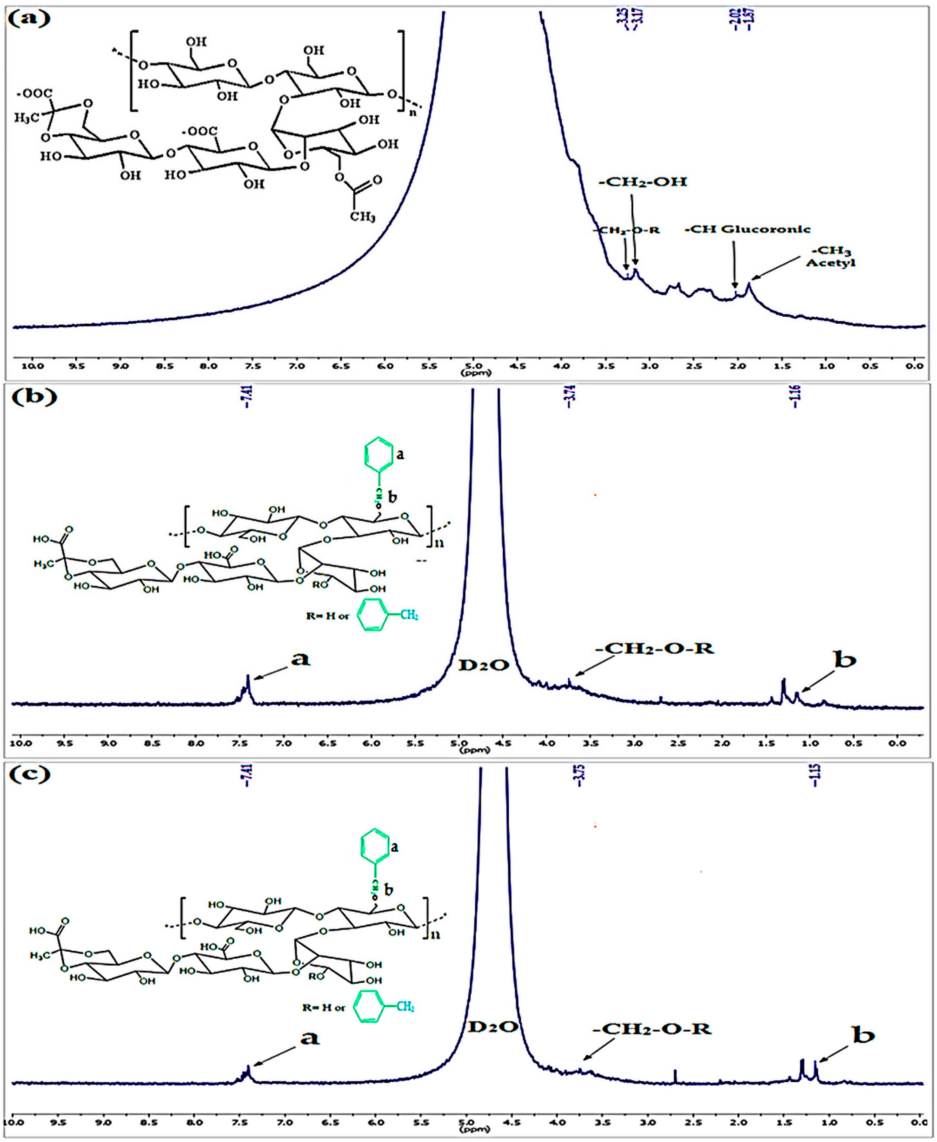

Figure 3. ^{1}H-NMR spectra of (**a**) XG, (**b**) BXG1, and (**c**) BXG2.

After modification, the ^{1}H-NMR analysis showed the disappearance of the peak at 1.87 ppm in the BXG1 and BXG2 spectra, indicating xanthan gum deacetylation due to the alkaline conditions of the Williamson synthesis. Furthermore, the apparition of new peaks was also observed on the BXG1 and BXG2 spectra assigned to the methylene (CH_2) protons that were detected at 1.16 and 1.15 ppm for BXG1 and BXG2, respectively [10,23]. Moreover, the peaks appearing at 7.41 ppm were attributed to the aromatic protons (C-H) [43,44].

Similar findings were reported by Skender et al. [34] for hydrophobically modified xanthan gum by the grafting of three different aromatic groups. Finally, the ^{1}H-NMR spectra of the two derivatives display the peaks of the methyl protons connected with the ether function (-CH_2-O-R), located at 3.74 ppm for BXG1 and 3.75 ppm for BXG2, which indicated successful etherification of native xanthan gum. Similar results (3.25 ppm) were found by Quan et al. [22].

3.3. Morphological Analysis

The morphological proprieties of xanthan gum (XG) and its benzyl derivatives are presented in Figure 4. The XG photomicrographs (Figure 4(a1,a2)) exhibit a smooth surface and the polyhedral granules present a rigid rod-like structure [23]. The BXGs micrographs showed a rougher surface of the granules and a decrease in particle size in addition to a more structured morphology in the form of semi-crystalline granules [35]. These results indicated that the benzylation reaction in the NaOH aqueous solution changed the surface of XG without denaturing its structural molecular backbone but it contributes to the formation of more homogeneously dispersed aggregates. The NaOH aqueous solution disrupted the intermolecular and intramolecular hydrogen bonds, leading to the formation of slightly smaller aggregates. Contrary to the results found by Sara et al. [23] with long-chain octyl xanthan gum derivatives, the particles of benzyl derivatives are smaller than those of xanthan gum but more agglomerated and more homogenously granulated. This may be explained by the fact that stronger hydrophobic interactions are formed between the aromatic moieties, leading to the formation of a denser structural network. The results obtained by Quan et al. [22] also demonstrated that the hydrophobic modification of xanthan gum led to the formation of a denser structural network without the denaturation of the structure. Additionally, microwave treatment is known to be more homogeneous, selective, and efficient and also results in faster reactions without affecting the original structure and physicochemical characteristics of the polysaccharide, as described by Desbrières et al. [27].

3.4. X-ray Diffraction (XRD)

The X-ray patterns of the native biopolymer (XG) and its benzylated derivatives are shown in Figure 5. For XG, the amorphous character was demonstrated [11]. However, the diffractograms of BXGs indicated their semi-crystallin structure with the apparition of characteristic sharp peaks at 2θ equal to 18.89°, 20.71°, and 22.87° for BXG1 that corresponded to 42.7%, 76.9%, and 41.2% intensity, and at 2θ values of 18.75°, 29.10°, 34.07°, and 45.13° for BXG2 that corresponded to 16.9%, 20.7%, 20.7%, 63.6%, and 19.4%. These results are following those reported by Toumi et al. [10] and Hamiouda et al. [23]. Indeed, the obtained degree of crystallinity (DOC) values of XG, BXG1, and BXG2 were 8.46%, 10.18%, and 14.67%, respectively. These results showed that the etherification with benzyl chloride results in a slight increase in crystallinity, but also demonstrated that the molecular structure of xanthan gum did not undergo denaturation due to the fact that the amorphous nature remains preponderant.

3.5. Rheological Study

The rheograms of xanthan gum and its benzylated (BXGs) derivatives at the concentrations of 0.5 and 1% are shown in Figure 6. It was noticed that the viscosity of XG is higher than those of BXGs ($p < 0.05$), this could be attributed to the decrease in molecular weight caused by the removal of acetyl groups by the deacetylation effect during the etherification process due to the alkaline treatment [23]. Moreover, it was observed that the flow curve tendencies of BXGs are similar to those of native xanthan, with the presence of two distinct regions: region (I) at very low shear rates, corresponding to the Newtonian plateau, and region (II), where the XG and its derivatives behave as pseudo-plastic fluids at high shear rates because of the orientation of macromolecules in the direction of flow or the molecular destructuring under the shear effect [11,45]. Furthermore, it was noted that the

viscosity increased with the substitution degree and concentration ($p < 0.05$). These results may be explained by the fact that the aromatic benzyl groups enhance the Van der Waals interactions among the chains of XG. This leads to the appearance of more interweaved segments between the molecular chains and an increase in internal flow resistance. These results are particularly interesting at the two relatively low concentrations of 0.5 and 1% in comparison to the solution of cholesteryl derivatives of mannan and pullulan, for which a pronounced shear-thinning behavior was observed at the concentrations equal to 12.5% and 8%, respectively [46].

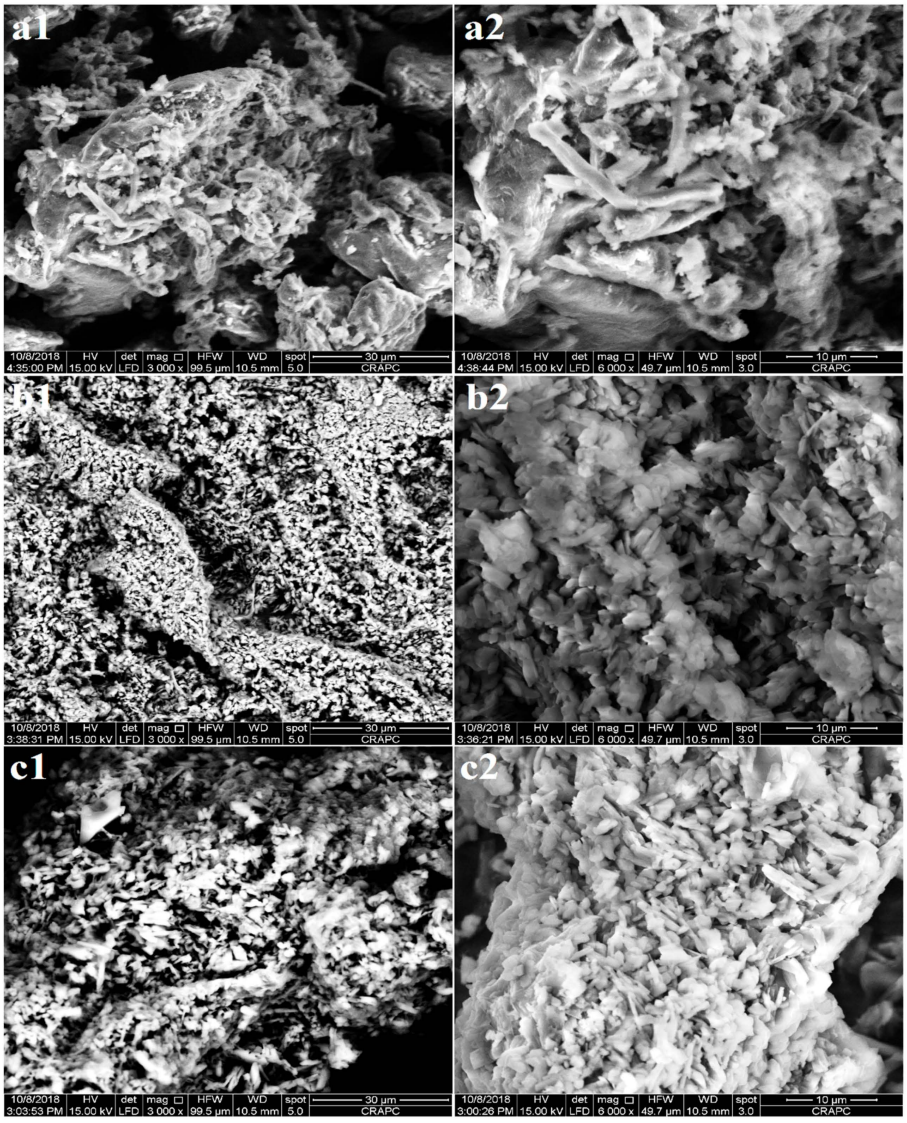

Figure 4. SEM photomicrographs at magnifications of XG (**a1**,**a2**), BXG2 (**b1**,**b2**), and BXG1 (**c1**,**c2**).

Oscillatory tests under deformation conditions were performed to analyze the linear viscoelastic properties of the aqueous solutions of XG and its benzylated derivatives. The obtained results describing the variations in XG and BXGs elastic (G′) and viscous (G″) moduli are presented in Figure 7. In the linear viscoelastic region (LVR), the native xanthan gum demonstrates a dominant elastic rather than viscous character, where the storage modulus was greater than the loss modulus (G′ > G″) that remains constant throughout the range of 0.01% to 60% ($p < 0.05$). This is typically characteristic of the solid gel-like behavior of native xanthan gum [9,23]. Moreover, BXG1 did not show any elastic or semi-solid behavior, as G″ > G′ along the whole strain sweep γ (%) and presents much lower values of the elastic modulus G′ ($p < 0.05$). This may be due to the deacetylation process caused

by the alkaline treatment. Additionally, the lower degree of substitution of BXG1 does not make it possible to form sufficiently strong inter-intramolecular hydrophobic interactions to compensate enough for the drop in viscosity resulting from slight depolymerization of the macromolecular chains. However, it seems that BXG2 behaves like XG with an elastic modulus reduced to lower values ($p < 0.05$) that can be due to the slight removal of the acetyl groups, as previously reported by Wu et al., who observed that high-acetyl xanthan has a higher G′ than low-acetyl xanthan [47], but its LVR region was located in the range of 0.01% to 6%. Finally, it was demonstrated that both the elastic and the viscous moduli of the two derivatives BXG1 and BXG2 increased with increasing DS [11].

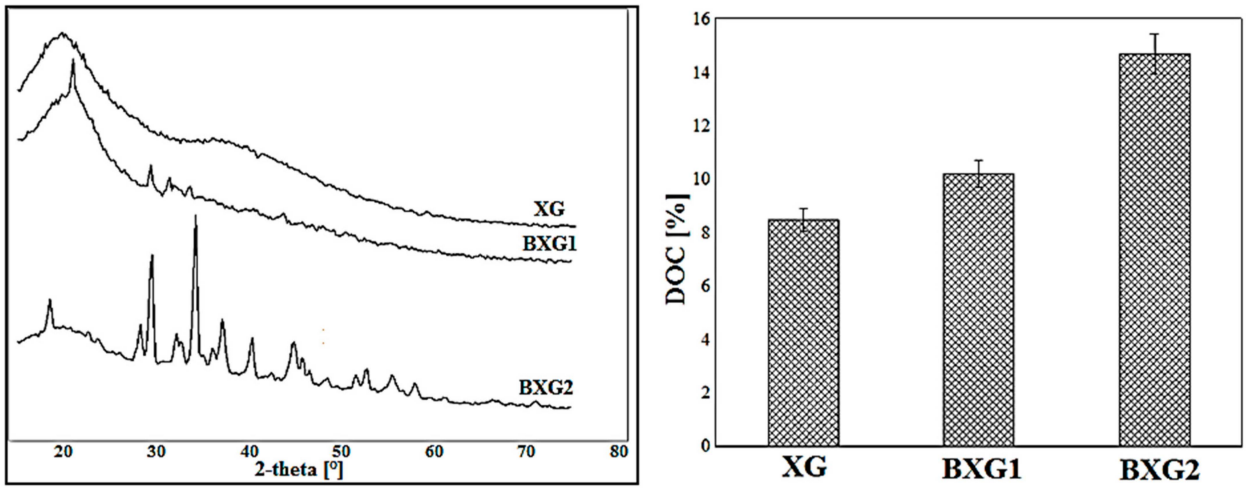

Figure 5. X-ray diffraction patterns (**left**) and DOC (**right**) for XG and BXGs.

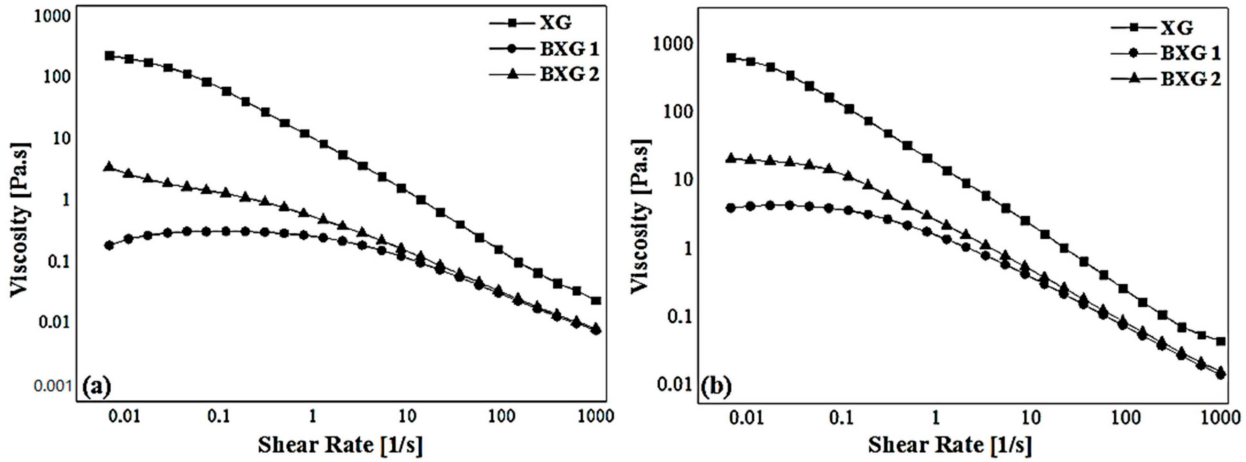

Figure 6. Flow curves of XG and its derivatives at concentrations of 0.5% (**a**) and 1% (**b**).

3.6. Viscosity-Average Molecular Weight Determination

The results of the average molecular weight determination (Mw) are illustrated in Figure 8, where it is shown that native xanthan gum presented an average molecular weight of 1.84962×10^6 g·mol^{-1} that was superior to those of BXG1 (1.37315×10^6 g·mol^{-1}) and BXG2 (1.27504×10^6 g·mol^{-1}). The molecular weight decreased after modification because of the deacetylation in the alkaline medium that reduced the number of acetyl groups in the biopolymer and, consequently, decreased its weight ($p < 0.05$). These results are in accordance with Khouryieh et al. [48] for deacetylated xanthan gum, Hamiouda et al. [23] for hydrophobically modified xanthan gum, and also Toumi et al. [10], for alkylated kappa-carrageenan, where NaOH strong alkaline solutions were used for the activation of the -OH groups in all of these works. Toumi et al. [10] revealed that the decrease in Mw of alkylated

kappa-carrageenan during the modification was also due to slight depolymerization of the polymeric chains through the β-(1–4) glycosidic bond cleavage during etherification [49]. However, Sawada et al. [50] found that cholesterol self-assembled derivatives of xyloglucan presented higher molecular weights (about 2×10^7 g/mol) than that of xyloglucan (about 2×10^5 g/mol). This may be the result of the operating conditions of the synthesis in anhydrous DMSO media using anhydrous Pyridine rather than NaOH, which is a stronger base.

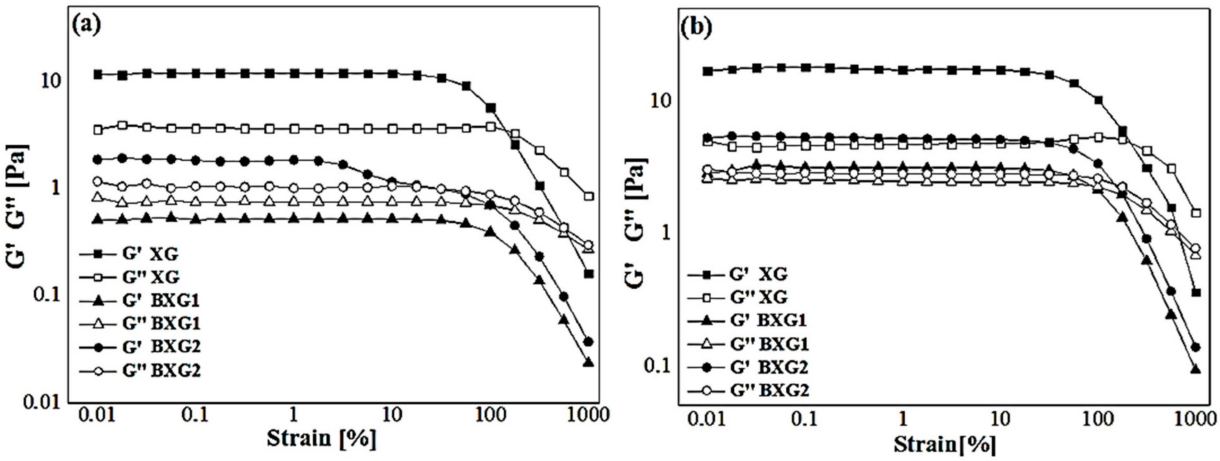

Figure 7. Strain sweep dependency of storage (G′) and loss (G″) moduli of XG and its BXG derivatives at concentrations of (**a**) 0.5% and (**b**) 1% at 1 Hz and 25 °C.

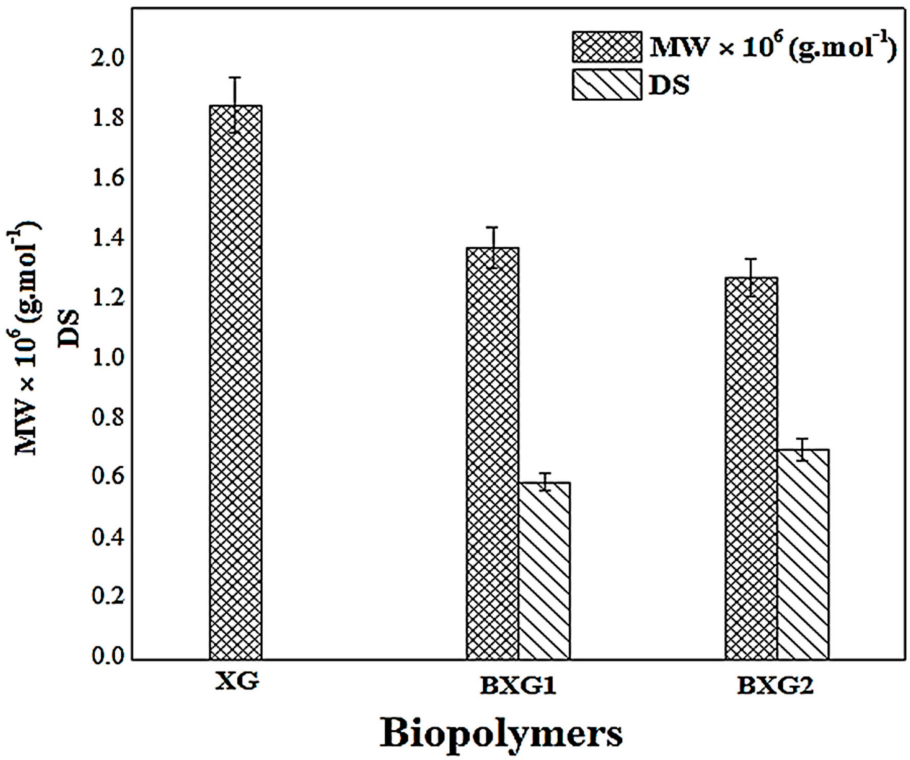

Figure 8. Variation of the degree of substitution (DS) and the molecular weight (Mw) of xanthan gum and its derivatives.

Furthermore, the Mw increased with the increased DS ($p < 0.05$), indicating the insertion of a greater number of aromatic groups onto the backbone of XG in BXG2 compared with BXG1 [10,38].

3.7. Critical Aggregation Concentration by Conductivity Measurements

Figure 9 represents the results of the conductivity measurements as a function of the concentration of BXG solutions. It is depicted that BXG2 showed higher conductivity values than BXG1 ($p < 0.05$). These results may be explained by the fact that, in an aqueous medium, the hydrophobic aromatic groups would inter-associate and form hydrophobic aggregates and therefore repulse the hydrophilic parts into the aqueous medium, which leads to the increasing conductivity values [39]. Furthermore, the obtained results showed that the conductivity plots exhibit two distinct regions separated by an inflection point. This point corresponds to the critical aggregation concentration (CAC) that is detected at 0.32% for BXG1 and 0.28% for BXG2. It is observed that the CAC decreases with the degree of substitution where the BXG2 derivative presents the lower value, which is probably caused by the increasing grafting rate of the hydrophobic benzyl groups ($p < 0.05$). The aggregation of amphiphilic polymers is controlled by the balance between the interaction of the hydrophobic groups and the hydrophilic chains. The presence of hydrophobic moieties on the flexible chains of xanthan gum leads to amplifying their capacity to self-associate in aqueous media through intra-and/or intermolecular interactions between the hydrophobic groups [30,31].

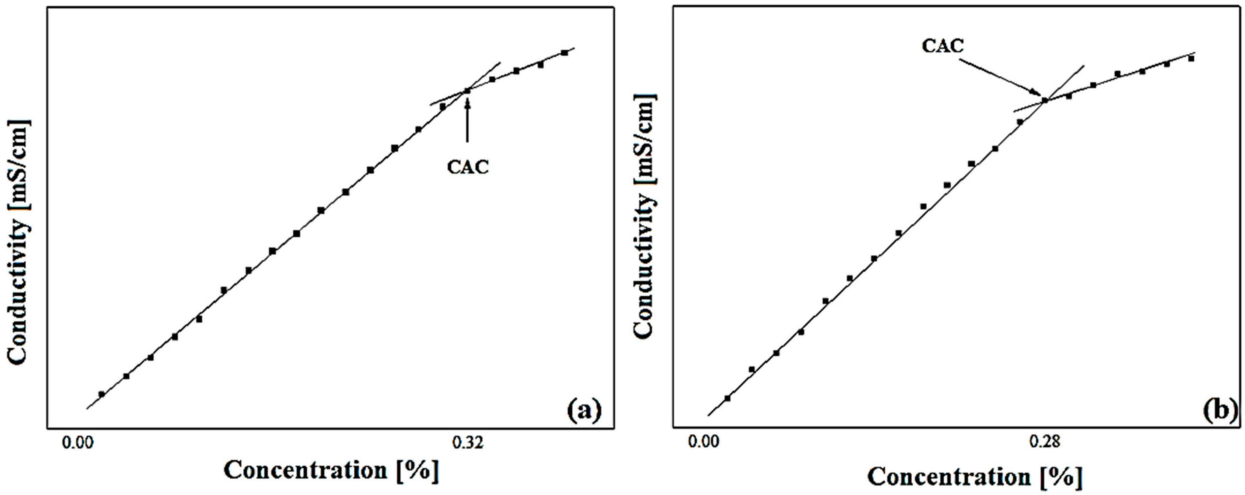

Figure 9. Conductivity determination of the CAC for BXG1 (**a**) and BXG2 (**b**).

At relatively high DS, higher intermolecular associations of polymers are induced through the association of hydrophobic groups, resulting in a remarkable decrease in CAC value. Our findings are in accordance with those found by Sara et al. [23] and Toumi et al. [10].

3.8. Emulsifying Study

For the emulsification study, emulsions were prepared based on XG and BXGs at two concentrations of 0.5 and 1%. However, only the 1% biopolymer emulsions were retained because they had greater stability and better macroscopic and microscopic characteristics. Indeed, the prepared emulsions at 0.5% remained stable barely 7 days after preparation and lead to the apparition of phase separation by the oil droplets' migration. This may be due to an insufficient amount of BXGs in the aqueous phase, which is not enough to allow stabilization of a large surface area and, thus, large droplets are finally obtained, leading to the occurrence of coalescence as described by Fantou et al. [51].

3.8.1. Macroscopic and Microscopic Aspects

The macroscopic characteristics of all the developed formulas, based on 1% (w/v) of polymer concentration, were determined immediately after the preparation using visual control. Figure 10 clearly shows the yellowish color of the emulsions obtained, which all

exhibit a homogeneous appearance with the absence of any form of apparent instability as well as a viscous and creamy consistency.

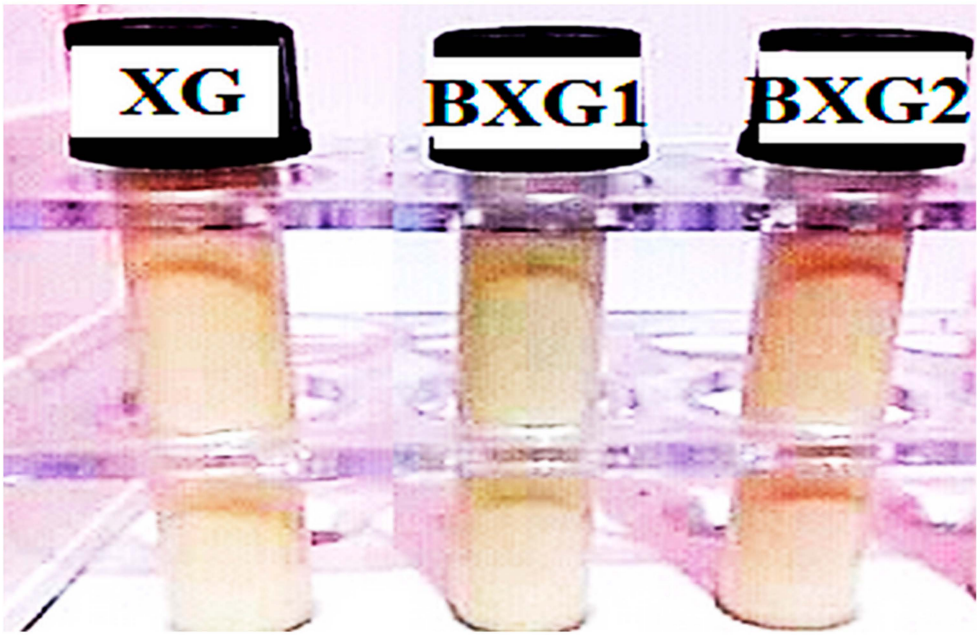

Figure 10. Photography of the emulsions based on: XG (F1), BXG1 (F2), and BXG2 (F3) at 1%.

The microstructures of the oil/water emulsions stabilized by native XG and its BXG derivatives at the polymer fraction of 1% are illustrated in Figure 11. It was observed that XG-based emulsion (F1) showed the inhomogeneous dispersion of particles and a higher particle size (42.5 µm), indicating that native XG had no interfacial activity [51]. Moreover, the BXG2-based formula (F3) presented a lower globule size (3.5 µm) and showed a uniform and more homogeneous particle distribution than those stabilized by BXG1 (F2) and XG (F1) ($p < 0.05$). It was concluded that the grafting of more hydrophobic fragments on a hydrophilic backbone of XG enhances its oil affinity and emulsification capacity. It also results in reduced size of the oil droplets and improves the stability of the emulsions [52]. These results are totally in accordance with the literature [38,39,43].

3.8.2. Accelerated Stability Testing

The accelerated stability testing results after a forced destabilization by centrifugation are represented in Table 2, where it is observed that the emulsions F3 based on BXG2 exhibit greater stability than those of the emulsions stabilized with BXG1 (F2) and XG (F1). The significant resistance of BXG2-based emulsions to accelerated destabilization confirmed the emulsifying potential of this derivative resulting from its higher degree of substitution (DS) value related to the number of benzyl hydrophobic moieties onto the native XG molecule, which improved its amphiphilic character.

Table 2. Results of the stability testing by centrifugation of emulsions stabilized with native xanthan gum and its hydrophobic derivatives BXG1 and BXG2.

Emulsions	Time (min)					
	5	10	15	20	25	30
F1	+	+	+	+	−	−
F2	+	+	+	+	+	−
F3	+	+	+	+	+	+

(+): Stable emulsions, (−): Unstable emulsions.

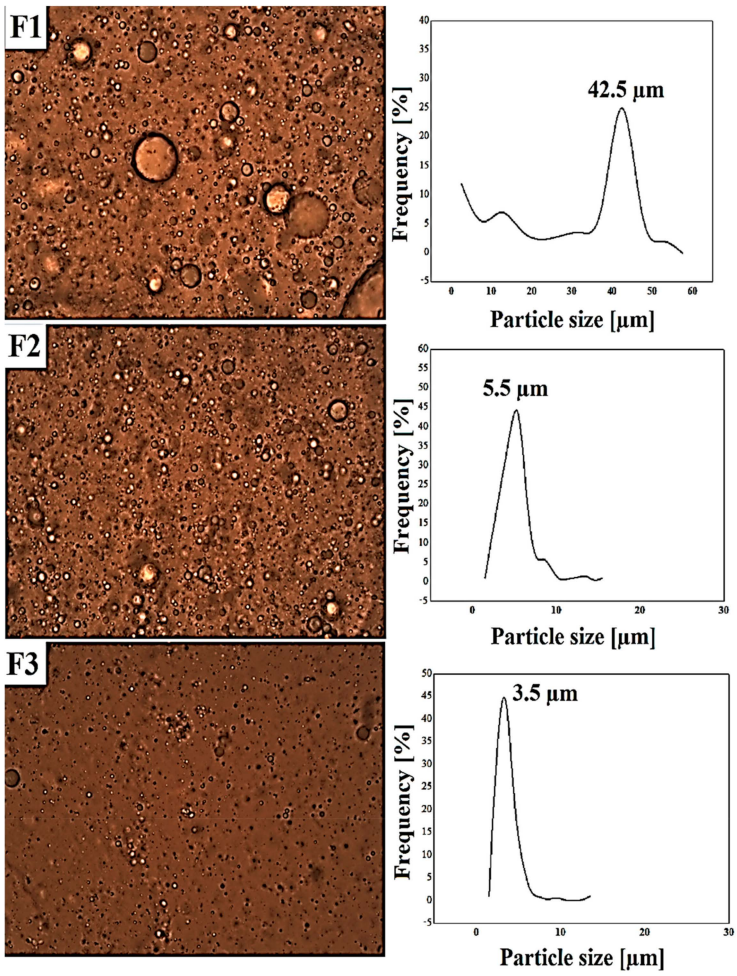

Figure 11. Photomicrographs and particle size distribution of the emulsions F1, F2, and F3 stabilized by XG, BXG1, and BXG2, respectively, at (40×) magnification after 24 h.

Indeed, when the amphiphilic character of the molecule is improved, it promotes the formation of a more rigid interfacial film surrounding the oil droplets and this, added to the viscosifying nature of these polysaccharides, will make it possible to slow down the diffusion of these globules, thus prolonging the emulsion stability. Analogous results were found by Hamiouda et al. for hydrophobically modified XG [23] and Toumi et al. [10,40] for alkylated kappa carrageenan and Osa kappa carrageenan.

4. Conclusions

New amphiphilic derivatives of xanthan gum were exclusively synthesized by an etherification reaction under microwave heating using benzyl chloride at two different reagent/polymer ratios of 2 and 6. Then, the two benzyl xanthan gum derivatives, BXG1 and BXG2, underwent preliminary physicochemical characterization for grafting confirmation and structural analysis. First, both FTIR and H^1-NMR analysis demonstrated the effectiveness of the hydrophobic modification and confirmed the grafting of the aromatic moieties onto the backbone of xanthan gum. Then, the physicochemical testing results showed slight and interesting modifications in the structural characteristics of the new derivatives and the conservation of the pseudoplastic shear-thinning behavior after hydrophobization, as well as the associative character of BXGs. The amphiphilic properties of BXGs were assessed by CAC determination, where the CAC values of 0.32% and 0.28% for BXG1 and BXG2 were obtained, respectively. An emulsification test was also performed to confirm the amphiphilic character of BXGs by the evaluation of emulsifying power. Then, the ability of the two BXG derivatives to stabilize oil/water emulsions was confirmed at the

biopolymer concentration of 1%. The results showed that the new benzylated XG derivatives exhibited promising stabilizing power, which is more pronounced for the derivative BXG2, having a higher degree of substitution (0.70) than BXG1, which had a lower DS value of 0.59. The XRD patterns of both XG and BXGs revealed a slight semi-crystalline aspect of the benzylated derivatives compared to the amorphous character of XG. Furthermore, these results were confirmed by the calculation of the degree of crystallinity (DOC) values which were 8.46%, 10.18%, and 14.67% for XG, BXG1, and BXG2, respectively.

Such synthesis under microwave heating constitutes a smart strategy. Microwave heating constitutes a cost-effective, environment-friendly, cleaner, and greener approach for biopolymer modification. Such an alternative results in greater control and higher reproducibility in the final product.

Finally, these findings are very encouraging and show the great potential of the novel BXG derivatives to be used as a thickening and stabilizing agent in many fields of industry and particularly in painting, pasting, and oil drilling formulations.

Author Contributions: Conceptualization, M.M.Y., S.T. and S.L.; methodology, M.M.Y., S.T., S.L. and A.H.; software, S.T., H.T. and S.L.; validation and supervision, S.L.; investigation, M.M.Y. and S.L. and A.H.; writing—original draft preparation, M.M.Y., S.T. and S.L.; writing—review and editing, S.L., M.M.Y. and S.T.; visualization, H.T., M.K., A.A., A.A.A., J.Z. and L.M.; Resources, H.T., M.K., A.A., A.A.A., J.Z. and L.M.; project administration, S.L. All authors have read and agreed to the published version of the manuscript.

Funding: This research received no external funding.

Institutional Review Board Statement: Not applicable.

Informed Consent Statement: Not applicable.

Data Availability Statement: The data presented in this study are available in the manuscript.

Conflicts of Interest: The authors declare no conflict of interest.

References

1. Xu, L.; Gong, H.; Dong, M.; Li, Y. Rheological Properties and Thickening Mechanism of Aqueous Diutan Gum Solution: Effects of Temperature and Salts. *Carbohydr. Polym.* **2015**, *132*, 620–629. [CrossRef] [PubMed]
2. Lefnaoui, S.; Moulai-Mostefa, N. Formulation and in Vitro Evaluation of K-carrageenan-pregelatinized Starch-based Mucoadhesive Gels Containing Miconazole. *Starch-Stärke* **2011**, *63*, 512–521. [CrossRef]
3. Wen, Y.; Yuan, Y.; Chen, H.; Xu, D.; Lin, K.; Liu, W. Effect of Chitosan on the Enantioselective Bioavailability of the Herbicide Dichlorprop to Chlorella Pyrenoidosa. *Environ. Sci. Technol.* **2010**, *44*, 4981–4987. [CrossRef] [PubMed]
4. Raigond, P.; Ezekiel, R.; Raigond, B. Resistant Starch in Food: A Review. *J. Sci. Food Agric.* **2014**, *95*, 1968–1978. [CrossRef] [PubMed]
5. Lefnaoui, S.; Moulai-Mostefa, N. Investigation and Optimization of Formulation Factors of a Hydrogel Network Based on Kappa Carrageenan–Pregelatinized Starch Blend Using an Experimental Design. *Colloids Surf. A Physicochem. Eng. Asp.* **2014**, *458*, 117–125. [CrossRef]
6. Mafi, R.; Pelton, R.; Cui, Y.; Ketelson, H. Weak Gelation of Hydrophobic Guar by Albumin in Simulated Human Tear Solutions. *Biomacromolecules* **2014**, *15*, 4637–4642. [CrossRef]
7. Lefnaoui, S.; Moulai-Mostefa, N.; Yahoum, M.M.; Gasmi, S.N. Design of Antihistaminic Transdermal Films Based on Alginate–Chitosan Polyelectrolyte Complexes: Characterization and Permeation Studies. *Drug Dev. Ind. Pharm.* **2018**, *44*, 432–443. [CrossRef]
8. Alquraishi, A.A.; Alsewailem, F.D. Xanthan and Guar Polymer Solutions for Water Shut off in High Salinity Reservoirs. *Carbohydr. Polym.* **2012**, *88*, 859–863. [CrossRef]
9. Lefnaoui, S.; Moulai-Mostefa, N. Synthesis and Evaluation of the Structural and Physicochemical Properties of Carboxymethyl Pregelatinized Starch as a Pharmaceutical Excipient. *Saudi Pharm. J.* **2015**, *23*, 698–711. [CrossRef] [PubMed]
10. Toumi, S.; Yahoum, M.M.; Lefnaoui, S.; Hadjsadok, A. Synthesis, Characterization and Potential Application of Hydrophobically Modified Carrageenan Derivatives as Pharmaceutical Excipients. *Carbohydr. Polym.* **2021**, *251*, 116997. [CrossRef]
11. Yahoum, M.M.; Moulai-Mostefa, N.; Le Cerf, D. Synthesis, Physicochemical, Structural and Rheological Characterizations of Carboxymethyl Xanthan Derivatives. *Carbohydr. Polym.* **2016**, *154*, 267–275. [CrossRef] [PubMed]
12. Jansson, P.-E.; Kenne, L.; Lindberg, B. Structure of the Extracellular Polysaccharide from Xanthomonas Campestris. *Carbohydr. Res.* **1975**, *45*, 275–282. [CrossRef]
13. Katzbauer, B. Properties and Applications of Xanthan Gum. *Polym. Degrad. Stab.* **1998**, *59*, 81–84. [CrossRef]

14. Garcıa-Ochoa, F.; Santos, V.E.; Casas, J.A.; Gómez, E. Xanthan Gum: Production, Recovery, and Properties. *Biotechnol. Adv.* **2000**, *18*, 549–579. [CrossRef]
15. Zheng, M.; Lian, F.; Zhu, Y.; Liu, B.; Chen, Z.; Zhang, Y.; Zheng, B.; Zhang, L. Modified Xanthan Gum for Crystal Violet Uptake: Kinetic, Isotherm, and Thermodynamic Behaviors. *Water Sci. Technol.* **2019**, *79*, 165–174. [CrossRef] [PubMed]
16. Ahuja, M.; Kumar, A.; Singh, K. Synthesis, Characterization and in Vitro Release Behavior of Carboxymethyl Xanthan. *Int. J. Biol. Macromol.* **2012**, *51*, 1086–1090. [CrossRef] [PubMed]
17. Makhado, E.; Pandey, S.; Nomngongo, P.N.; Ramontja, J. Fast Microwave-Assisted Green Synthesis of Xanthan Gum Grafted Acrylic Acid for Enhanced Methylene Blue Dye Removal from Aqueous Solution. *Carbohydr. Polym.* **2017**, *176*, 315–326. [CrossRef] [PubMed]
18. Zheng, M.; Lian, F.; Xiong, Y.; Liu, B.; Zhu, Y.; Miao, S.; Zhang, L.; Zheng, B. The Synthesis and Characterization of a Xanthan Gum-Acrylamide-Trimethylolpropane Triglycidyl Ether Hydrogel. *Food Chem.* **2019**, *272*, 574–579. [CrossRef]
19. Hassani, L.N.; Hendra, F.; Bouchemal, K. Auto-Associative Amphiphilic Polysaccharides as Drug Delivery Systems. *Drug Discov. Today* **2012**, *17*, 608–614. [CrossRef]
20. Riaz, T.; Iqbal, M.W.; Jiang, B.; Chen, J. A Review of the Enzymatic, Physical, and Chemical Modification Techniques of Xanthan Gum. *Int. J. Biol. Macromol.* **2021**, *186*, 472–489. [CrossRef]
21. Fantou, C.; Roy, A.N.; Dé, E.; Comesse, S.; Grisel, M.; Renou, F. Chemical Modification of Xanthan in the Ordered and Disordered States: An Open Route for Tuning the Physico-Chemical Properties. *Carbohydr. Polym.* **2017**, *178*, 115–122. [CrossRef] [PubMed]
22. Quan, H.; Hu, Y.; Huang, Z.; Wenmeng, D. Preparation and Property Evaluation of a Hydrophobically Modified Xanthan Gum XG-C16. *J. Dispers. Sci. Technol.* **2019**, *41*, 656–666. [CrossRef]
23. Sara, H.; Yahoum, M.M.; Lefnaoui, S.; Abdelkader, H.; Moulai-Mostefa, N. New Alkylated Xanthan Gum as Amphiphilic Derivatives: Synthesis, Physicochemical and Rheological Studies. *J. Mol. Struct.* **2020**, *1207*, 127768. [CrossRef]
24. Wang, X.; Xin, H.; Zhu, Y.; Chen, W.; Tang, E.; Zhang, J.; Tan, Y. Synthesis and Characterization of Modified Xanthan Gum Using Poly (Maleic Anhydride/1-Octadecene). *Colloid Polym. Sci.* **2016**, *294*, 1333–1341. [CrossRef]
25. Wu, Z.; Li, H.; Zhao, X.; Ye, F.; Zhao, G. Hydrophobically Modified Polysaccharides and Their Self-Assembled Systems: A Review on Structures and Food Applications. *Carbohydr. Polym.* **2022**, *284*, 119182. [CrossRef]
26. Wong, T.; Brault, L.; Gasparotto, E.; Vallée, R.; Morvan, P.-Y.; Ferrières, V.; Nugier-Chauvin, C. Formation of Amphiphilic Molecules from the Most Common Marine Polysaccharides, toward a Sustainable Alternative? *Molecules* **2021**, *26*, 4445. [CrossRef] [PubMed]
27. Desbrières, J.; Petit, C.; Reynaud, S. Microwave-Assisted Modifications of Polysaccharides. *Pure Appl. Chem.* **2014**, *86*, 1695–1706. [CrossRef]
28. García-Vaquero, M.; Rajauria, G.; O'Doherty, J.V.; Sweeney, T. Polysaccharides from Macroalgae: Recent Advances, Innovative Technologies and Challenges in Extraction and Purification. *Food Res. Int.* **2017**, *99*, 1011–1020. [CrossRef]
29. Xu, P.; Zheng, G.-W.; Zong, M.-H.; Li, N.; Lou, W.-Y. Recent Progress on Deep Eutectic Solvents in Biocatalysis. *Bioresour. Bioprocess.* **2017**, *4*, 34. [CrossRef]
30. Abou Dib, M.; Hucher, N.; Gore, E.; Grisel, M. Original Tools for Xanthan Hydrophobization in Green Media: Synthesis and Characterization of Surface Activity. *Carbohydr. Polym.* **2022**, *291*, 119548. [CrossRef]
31. Abou Dib, M.; Gore, E.; Grisel, M. Intrinsic and Rheological Properties of Hydrophobically Modified Xanthan Synthesized under Green Conditions. *Food Hydrocoll.* **2023**, *138*, 108461. [CrossRef]
32. Polêto, M.D.; Rusu, V.H.; Grisci, B.I.; Dorn, M.; Lins, R.D.; Verli, H. Aromatic Rings Commonly Used in Medicinal Chemistry: Force Fields Comparison and Interactions with Water toward the Design of New Chemical Entities. *Front. Pharmacol.* **2018**, *9*, 395. [CrossRef] [PubMed]
33. Selley, R.C.; Sonnenberg, S.A.; Sonnenberg, R. The Physical and Chemical Properties of Petroleum. In *Elements of Petroleum Geology*; Academic Press: Cambridge, MA, USA, 2015; pp. 13–39.
34. Skender, A.; Hadj-Ziane-Zafour, A.; Flahaut, E. Chemical Functionalization of Xanthan Gum for the Dispersion of Double-Walled Carbon Nanotubes in Water. *Carbon* **2013**, *62*, 149–156. [CrossRef]
35. Li, M.-F.; Sun, S.-N.; Xu, F.; Sun, R. Benzylation and Characterization of Cold NaOH/Urea Pre-Swelled Bamboo. *BioResources* **2012**, *7*, 1876–1890. [CrossRef]
36. Masuelli, M.A. Mark-Houwink Parameters for Aqueous-Soluble Polymers and Biopolymers at Various Temperatures. *J. Polym. Biopolym. Phys. Chem.* **2014**, *2*, 37–43.
37. Maity, S.; Sa, B. Ca-Carboxymethyl Xanthan Gum Mini-Matrices: Swelling, Erosion and Their Impact on Drug Release Mechanism. *Int. J. Biol. Macromol.* **2014**, *68*, 78–85. [CrossRef]
38. Tinland, B.; Rinaudo, M. Dependence of the Stiffness of the Xanthan Chain on the External Salt Concentration. *Macromolecules* **1989**, *22*, 1863–1865. [CrossRef]
39. Shahin, M.; Hady, S.A.; Hammad, M.; Mortada, N. Development of Stable O/W Emulsions of Three Different Oils. *Int. J. Pharm. Stud. Res.* **2011**, *2*, 45–51.
40. Toumi, S.; Yahoum, M.M.; Lefnaoui, S.; Hadjsadok, A. Synthesis and Physicochemical Evaluation of Octenylsuccinated Kappa-Carrageenan: Conventional versus Microwave Heating. *Carbohydr. Polym.* **2022**, *286*, 119310. [CrossRef]
41. Najafi, P.; Penchah, H.R.; Ghaemi, A. Synthesis and Characterization of Benzyl Chloride-Based Hypercrosslinked Polymers and Its Amine-Modification as an Adsorbent for CO_2 Capture. *Environ. Technol. Innov.* **2021**, *23*, 101746. [CrossRef]

42. Faria, S.; de Oliveira Petkowicz, C.L.; De Morais, S.A.L.; Terrones, M.G.H.; De Resende, M.M.; de Franca, F.P.; Cardoso, V.L. Characterization of Xanthan Gum Produced from Sugar Cane Broth. *Carbohydr. Polym.* **2011**, *86*, 469–476. [CrossRef]
43. Liebert, T.; Hänsch, C.; Heinze, T. Click Chemistry with Polysaccharides. *Macromol. Rapid Commun.* **2006**, *27*, 208–213. [CrossRef]
44. Hartman, J.; Albertsson, A.-C.; Sjöberg, J. Surface-and Bulk-Modified Galactoglucomannan Hemicellulose Films and Film Laminates for Versatile Oxygen Barriers. *Biomacromolecules* **2006**, *7*, 1983–1989. [CrossRef] [PubMed]
45. Barnes, H.A.; Hutton, J.F.; Walters, K. *An Introduction to Rheology*; Elsevier: Amsterdam, The Netherlands, 1989; Volume 3, ISBN 0-08-093369-6.
46. Akiyama, E.; Morimoto, N.; Kujawa, P.; Ozawa, Y.; Winnik, F.M.; Akiyoshi, K. Self-Assembled Nanogels of Cholesteryl-Modified Polysaccharides: Effect of the Polysaccharide Structure on Their Association Characteristics in the Dilute and Semidilute Regimes. *Biomacromolecules* **2007**, *8*, 2366–2373. [CrossRef]
47. Wu, M.; Qu, J.; Shen, Y.; Dai, X.; Wei, W.; Shi, Z.; Li, G.; Ma, T. Gel Properties of Xanthan Containing a Single Repeating Unit with Saturated Pyruvate Produced by an Engineered Xanthomonas Campestris CGMCC 15155. *Food Hydrocoll.* **2019**, *87*, 747–757. [CrossRef]
48. Khouryieh, H.A.; Herald, T.J.; Aramouni, F.; Bean, S.; Alavi, S. Influence of Deacetylation on the Rheological Properties of Xanthan–Guar Interactions in Dilute Aqueous Solutions. *J. Food Sci.* **2007**, *72*, C173–C181. [CrossRef]
49. Li, Y.J.; Ha, Y.M.; Wang, F.; Li, Y.F. Effect of Irradiation on the Molecular Weight, Structure and Apparent Viscosity of Xanthan Gum in Aqueous Solution. In *Advanced Materials Research*; Trans Tech Publications Ltd.: Stafa-Zurich, Switzerland, 2011; Volume 239, pp. 2632–2637.
50. Sawada, S.; Yukawa, H.; Takeda, S.; Sasaki, Y.; Akiyoshi, K. Self-Assembled Nanogel of Cholesterol-Bearing Xyloglucan as a Drug Delivery Nanocarrier. *J. Biomater. Sci. Polym. Ed.* **2017**, *28*, 1183–1198. [CrossRef]
51. Fantou, C.; Comesse, S.; Renou, F.; Grisel, M. Hydrophobically Modified Xanthan: Thickening and Surface-Active Agent for Highly Stable Oil in Water Emulsions. *Carbohydr. Polym.* **2019**, *205*, 362–370. [CrossRef]
52. Li, X.-M.; Zhu, J.; Pan, Y.; Meng, R.; Zhang, B.; Chen, H.-Q. Fabrication and Characterization of Pickering Emulsions Stabilized by Octenyl Succinic Anhydride-Modified Gliadin Nanoparticle. *Food Hydrocoll.* **2019**, *90*, 19–27. [CrossRef]